Sensitivity versus resonance in two-dimensional spiking-bursting neuron models

Borja Ibarz,[1,*] Gouhei Tanaka,[2,†] Miguel A. F. Sanjuán,[1] and Kazuyuki Aihara[3]

[1]*Nonlinear Dynamics and Chaos Group, Departamento de Física, Universidad Rey Juan Carlos, Tulipán s/n,
28933 Móstoles, Madrid, Spain*

[2]*Institute of Industrial Science, University of Tokyo, 153-8505, Tokyo, Japan*

[3]*Institute of Industrial Science, University of Tokyo, 153-8505, Tokyo, Japan
and ERATO Aihara Complexity Modeling Project, JST, 151-0065, Tokyo, Japan*

Through phase plane analysis of a class of two-dimensional spiking and bursting neuron models, covering some of the most popular map-based neuron models, we show that there exists a trade-off between the sensitivity of the neuron to steady external stimulation and its resonance properties, and how this trade-off may be tuned by the neutral or asymptotic character of the slow variable. Implications of the results for the suprathreshold behavior of the neurons, both by themselves and as part of networks, are presented in different regimes of interest, such as the excitable, regular spiking, and bursting regimes. These results establish a consistent link between single-neuron parameters and resulting network dynamics, and will hopefully be useful as a guide for modeling.

PACS number(s): 87.19.La, 05.45.−a, 05.45.Xt

INTRODUCTION

The response of a neuron to its inputs is determined by its subthreshold behavior. While for most applications the suprathreshold action potential can be simplified to a stereotyped response, subthreshold properties cannot be disregarded without compromising fundamental characteristics of the neuron such as sensitivity to external stimulation, refractoriness, oscillations, and resonance. Good neuronal modeling requires therefore attention to subthreshold dynamics and, understandably, much effort has been spent on the study and classification of the ionic currents involved and their mechanisms. The broad range of choices at the disposal of the modeler results in a need for general principles to guide the selection of the most appropriate for each specific purpose. To this end, the analysis of simplified or generic models has proved extremely useful [1].

The present paper is a contribution to the understanding of general dynamic constraints in neuron models. We concentrate on phenomenological models of the type that has been called resonate-and-fire [2] or generalized integrate-and-fire [3]. The subthreshold dynamics of these models is reduced to the minimum necessary for oscillations, that is, two variables, while the action potential generation is embodied in a simple threshold mechanism. Additionally, one of the variables, representing the neuronal membrane potential, evolves on a faster time scale than the other one. Our aim is to highlight the influence of one parameter upon neuron dynamics, and how it tunes the model between integrator and resonator behaviors [4].

The observation that triggered our study was the different behavior of two similar, recently proposed and already widely used neuron models, one by Rulkov [5] and the other by Izhikevich [6]. Phase plane analysis classifies both as resonators, because, for typical values of their parameters, they undergo a Neimark-Sacker bifurcation when pulled from their resting state by external excitation. But while the bifurcation of the former model is supercritical, and thus gives rise to self-sustained subthreshold oscillations, in the latter it is subcritical, and the neuron jumps directly from quiescence to full-blown spiking. We found that the supercritical behavior of the Rulkov model was due to the neutral character of the slow variable, as opposed to its asymptotic character in the Izhikevich model. But we also found that the parameter which allows us to tune this character—namely the slope of the slow nullcline—modified at the same time, in opposite directions, the sensitivity to external stimulation and the selectivity to its frequency. Thus our main conclusion, valid for a whole class of two-dimensional, fast-slow, spiking and bursting neuron models: The more sensitive the neuron is to external stimulation, the weaker its resonance properties are. This trade-off highlights the integrator versus resonator opposition.

Finally, since subthreshold properties are only important to the extent that they affect suprathreshold dynamics, we proceed to show the effects of the aforementioned trade-off on spike rate sensitivity to external currents, regularization of spike trains, synchronization, and propagation of activity in a network. We see, for example, that spontaneous synchronization in a network through electrical coupling is not enhanced by subthreshold resonance because of the reduced sensitivity that it entails.

Most of our discussion turns around map-based models instead of the more conventional models based on ordinary differential equations because we have been using them often in previous research [7,8] due to their computational advantages [9] and, more peculiarly, their chaotic properties. But nothing in the main results of the present paper is exclusive of discrete-time models, and in fact our analytical derivations will also be presented for their continuous-time counterparts.

*Electronic address: borja.ibarz@urjc.es

†Electronic address: gouhei@sat.t.u-tokyo.ac.jp

NEURON MODEL

We study a class of two-dimensional spiking-bursting neuron models that is captured by the following equations:

$$v(t+1) = F(v(t), I_v \pm u(t)),$$

$$u(t+1) = u(t) \mp pv(t) - qu(t) + I_u. \quad (1)$$

Variable v stands for transmembrane voltage, while u represents a depolarizing or hyperpolarizing current [depending on the sign chosen for the $\pm u(t)$ term, opposite for the $\mp pv(t)$ term], and is referred to as the recovery variable because of its role in ending bursts of action potentials. Parameters I_v and I_u are external inputs; I_v represents an injected current, while I_u modulates the dynamics of the recovery variable. Both p and q are positive and small parameters ($p, q \ll 1$), making u slow. This allows us to treat u as a parameter of the fast subsystem (variable v), and to predict its dynamics from average values of v.

The function $F(v, I_v \pm u)$ embodies the nonlinear mechanism for generation and reset of action potentials. It usually contains a discontinuity [the exception being the chaotic Rulkov model, Fig. 2(c)] that provides the threshold-and-reset mechanism that characterizes generalized integrate-and-fire models [3]. It is important to note that, except for this discontinuity, the second variable enters simply additively in $F(v, I_v \pm u)$, that is,

$$F(v, I_v \pm u) = f(v) + I_v \pm u.$$

We can thus understand the dynamics of v from the return map $f(v)$, shifted up or down by the slow variable u. Typically, low (for the plus sign) or high (for the minus sign) values of u produce a stable fixed point and the corresponding quiescence in the fast subsystem, while the opposite destroys the fixed point and gives rise to spiking. Cyclic variations in u allow the model to burst.

It is mainly through different forms of $f(v)$, along with particular choices of parameters p and q, that different variations of the class of models (1) are produced. Two well-known ones are those proposed by Rulkov [5,10,11] and Izhikevich [6,12]. Since we will be using them to show the implications of our analysis, and since they help understand the rationale behind the generic model (1), we present them in the following.

The Rulkov model has at least three variants: A simple bursting model [11], a bursting model with self-sustained subthreshold oscillations [5], and a chaotic bursting model [10]. We choose to present here the second one because subthreshold oscillations will be discussed in the following, and because its fast subsystem is locally equivalent to that of the Izhikevich model, which will make for a more interesting comparison between the two. The equations are

$$v(t+1) = F(v(t), I_v + u(t)),$$

$$u(t+1) = u(t) - \mu(v(t) + 1 - \sigma), \quad (2)$$

where

$$F(v, I_v + u)$$
$$= \begin{cases} -\dfrac{\alpha^2}{4} - \alpha + I_v + u, & \text{if } v < -1 - \dfrac{\alpha}{2}, \\[2mm] \alpha v + (v+1)^2 + I_v + u, & \text{if } -1 - \dfrac{\alpha}{2} \le v \le 0, \\[2mm] 1 + I_v + u, & \text{if } 0 < v < 1 + I_v + u, \\[2mm] -1, & \text{if } v \ge 1 + I_v + u. \end{cases} \quad (3)$$

Clearly the model corresponds to Eqs. (1) with $p = \mu \ll 1$, $q = 0$, and $I_u = \mu(1 - \sigma)$. The function $F(v, I_v + u)$, represented in Fig. 2(a), includes a nonlinear part responsible for spike initiation, and a reset mechanism for spikes. As explained before, the slow variable u and the external current I_v shift $F(v, I_v + u)$ vertically (except for the fixed reset level), provoking the creation or destruction of a pair of fixed points in the fast subsystem via a saddle-node bifurcation. The parameter α determines the position of these fixed points with respect to the reset level, and thus determines whether or not bursting is possible.

The interplay between the fast and slow subsystems will be best understood in terms of the nullcline diagram depicted in Fig. 1. The fast nullcline is a parabola whose branches, when the slow variable is treated as a parameter, can be classified as stable (N_s) and unstable (N_u), respectively. The vertex of the parabola is the aforementioned saddle-node bifurcation of the fast subsystem. For u values to the left of the vertex where these branches meet, the fast subsystem has two fixed points. One of them is stable and corresponds to the resting state of the neuron. If u goes beyond the vertex, the fixed points disappear; v then blows up until it reaches the value $1 + I_v + u$, at which it returns to the reset level $v = -1$ and starts again: The neuron is in the spiking regime. For its part, u increases when v is below the slow nullcline $v = -1 + \sigma$ and decreases otherwise. Thus if the orbit is below this nullcline, it will closely follow N_s towards the vertex. It will stop if it meets the point of intersection of N_s with the slow nullcline before passing the vertex. Otherwise, it will jump above, producing one or several action potentials.

If $\alpha > 1$, the vertex of the fast nullcline is below the reset value $v = -1$ and either bursting or tonic spiking, depending on the value of σ, is possible. Bursting will arise when, upon reset from a first spike, the orbit is above N_u; it then may produce a second spike, and so on. Meanwhile, u will gradually decrease until the orbit falls below N_u and the burst terminates.

The Rulkov system has only one stationary state O, at the intersection of the slow and fast nullclines. With $\mu \approx 0$, this state is stable if it lies on the stable branch N_s of the v nullcline, and unstable otherwise. The external input σ determines the position of the slow nullcline, and its variations provoke the gain or loss of stability of the fixed point through a Neimark-Sacker bifurcation. On the contrary, the external input I_v merely shifts the fast nullcline horizontally, failing to produce any change in its position relative to the slow nullcline. Therefore only transient changes in the state of the system take place in response to steady variations of
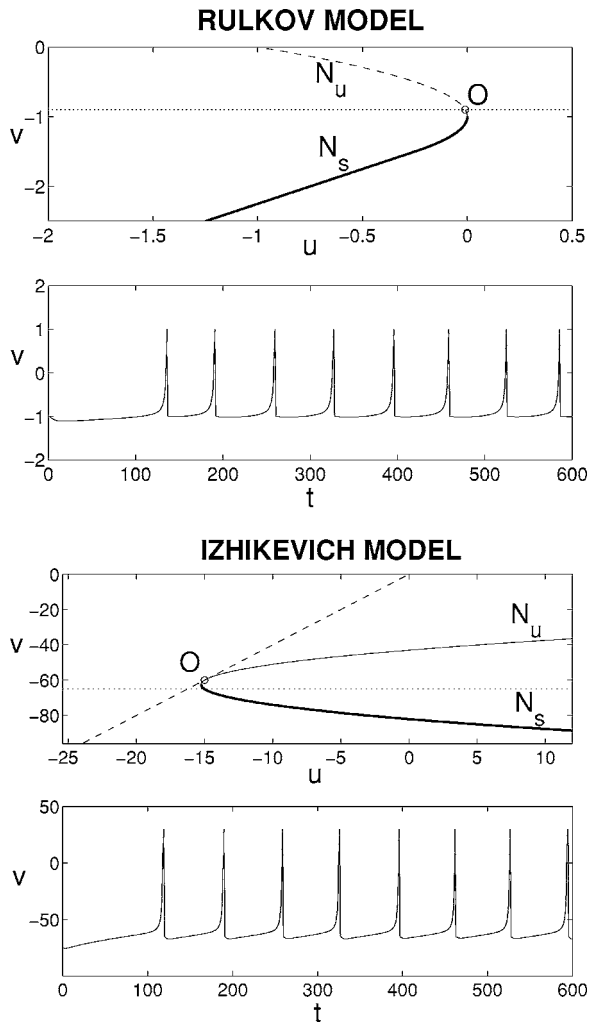
FIG. 1. Phase plane (above) and example of time evolution (below) of the Rulkov (top) and Izhikevich (bottom) models. See text for detailed explanation. Parameter values for the Rulkov model of Eqs. (2) are $\alpha=1.0$, $\mu=0.001$, $\sigma=0.1$, and $I_v=0$. Parameter values for the Izhikevich model of Eqs. (4) are $a=0.02$, $b=0.25$, $c=-65$, and $I_v=0.9$.

I_v. This observation is going to be central in the following discussion, since it helps explain why a horizontal slow nullcline entails reduced sensitivity to external currents.

The Izhikevich model is originally continuous time [6], but Euler discretization with a time step of 1 ms, as in [12], turns it into the map

$$v(t+1) = F(v(t), I_v - u(t)),$$

$$u(t+1) = u(t) + a(bv(t) - u(t)), \qquad (4)$$

where

$$F(v, I_v - u)$$
$$= \begin{cases} \min(0.04v^2 + 6v + 140 + I_v - u, 30) & \text{if} \quad v < 30, \\ c & \text{if} \quad v \ge 30. \end{cases}$$
$$(5)$$

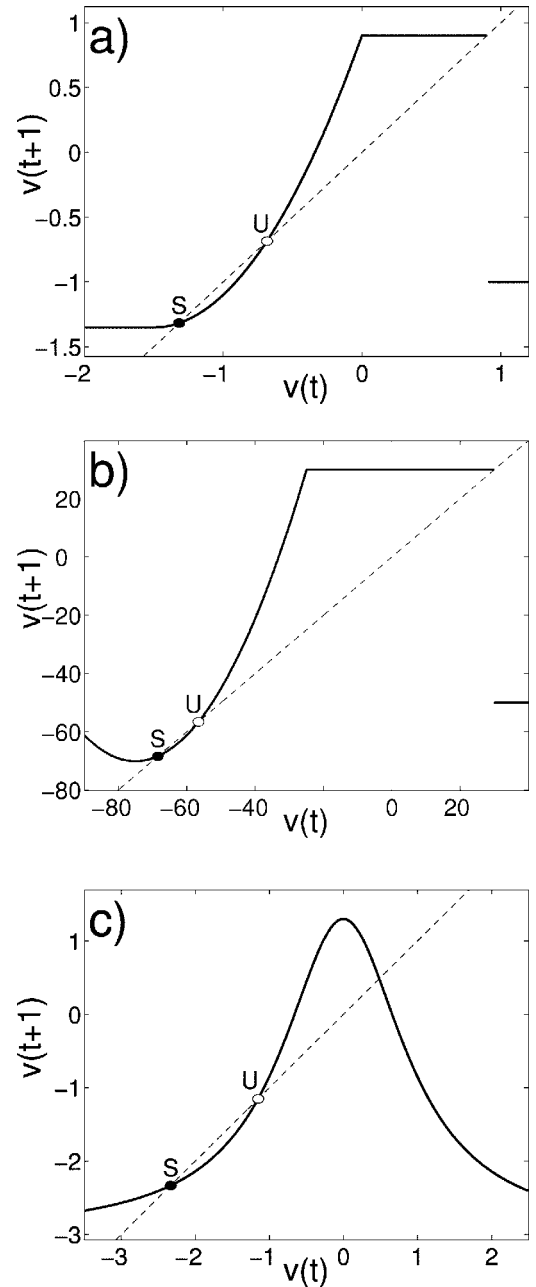Smaller time steps may be required depending on the appli-

FIG. 2. Functions $F(v, I_v \pm u)$ of (a) the Rulkov model with self-sustained subthreshold oscillations ($\alpha=1.0$, $I_v+u=-0.1$), (b) the Izhikevich model ($I_v-u=-15$), and (c) the chaotic Rulkov model ($\alpha=6.0$, $I_v+u=-3$). A value of $I_v \pm u$ has been chosen in each case that places the map below the saddle-node bifurcation, with stable (S) and unstable (U) fixed points. Variations in $I_v \pm u$ would shift these maps up or down, except for the reset branches in (a) and (b). Maps (a) and (b) are briefly explained in the present section, while the chaotic Rulkov model will be used later to illustrate chaotic itinerancy

cation, merely resulting in a scaling down of I_v, $F(v, I_v-u)$, u, and b. This would make no difference for our analysis.

The similarity with the Rulkov model is apparent in the nullcline diagram (Fig. 1) and in the return map of the fast subsystem (Fig. 2). Parameter a is small. The values of parameters of the generic model (1) that correspond to the

Izhikevich model are $p=ab \ll 1$, $q=a \ll 1$, and $I_u=0$. The slow variable u modulates the dynamics of the fast variable v, which represents transmembrane voltage. The fast nullcline has again a stable branch N_s and an unstable branch N_u, while the slow nullcline is a straight line. However, differing from the Rulkov model, this straight line is not horizontal, and therefore may cut the fast nullcline in two points. The nonzero slope means that the slow variable is asymptotically stable, while in the Rulkov model it is neutrally stable. Observe that, in this case, because the slow nullcline is slanted, variations of I_v, which shift the fast nullcline horizontally, do affect the relative position of the nullclines and can induce the Neimark-Sacker bifurcation that determines stability. Parameter c is the spike reset level and can be used, very much like the parameter α in the Rulkov model, to allow or forbid bursting, and to tune the duration of bursts and interburst intervals. Another parameter, d, used in the original model [6], will be zero always in this paper and for simplicity is ignored here.

The features of the models necessary for the validity of our analysis are the two-dimensionality of the phase space, the slow-fast dynamics, and the linearity of the slow variable. Their discrete-time nature, on the other hand, is not essential. We will see how the main results carry over to the corresponding continuous-time equations, which are

$$\tau \dot{v} = f(v) - v \pm u + I_v,$$

$$\tau \dot{u} = pv \mp qu + I_u. \tag{6}$$

The discrete-time model (1) can be retrieved from system (6) by Euler integration with time step τ. In continuous-time the reset mechanism cannot be subsumed in $f(v)$; it must be explicitly added as a jump condition, as in integrate-and-fire models. This is immaterial to the subthreshold analysis of the following section. The sensitivity versus resonance trade-off, and its implications for spiking and bursting, hold both in discrete and continuous time. Only the effects upon the chaotic model, presented at the end of the paper, have no continuous-time counterpart.

ANALYSIS OF SENSITIVITY AND RESONANCE

In this section we use phase plane and bifurcation analysis to demonstrate the sensitivity versus resonance trade-off in the family of models presented in the preceding section. The trade-off stems from the fact that a single parameter, namely the slope of the slow variable nullcline, controls both features. We perform the analysis on the generic model (1) (or its continuous-time counterpart), where the nullcline slope is q/p. When a particular choice of $f(v)$ is needed, we illustrate the results with the Izhikevich model, which allows us to tune the slope $1/b$, or the Rulkov model, which represents the extreme case of zero slope.

Sensitivity to external currents

By sensitivity in a neuron we understand the magnitude of its response to external inputs. A typical measure of this is the gain function [13], defined as the dependence of the fir-
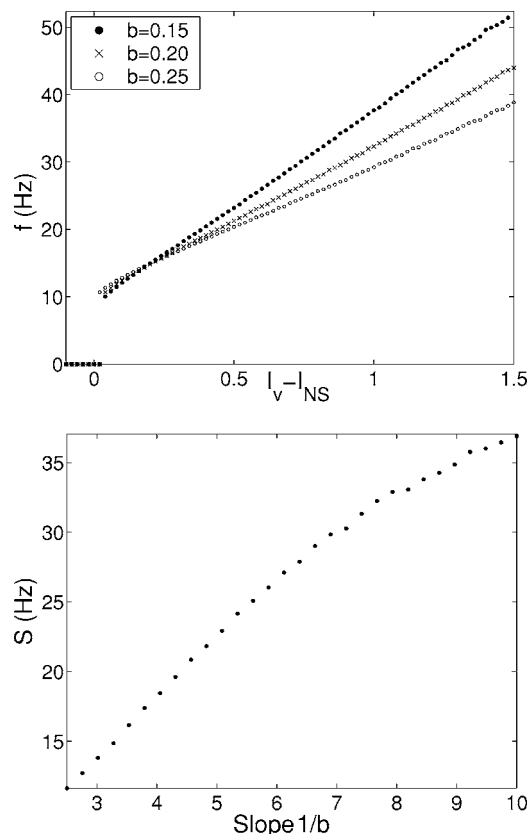

FIG. 3. Top: Gain function of the Izhikevich model for three different values of b. Currents I_v are referred to the level I_{NS} of loss of stability of the fixed point. Bottom: Sensitivity of the Izhikevich model, measured as the increase in firing rate per external current unit (regression average for I_v between $I_{NS}+0.5$ and $I_{NS}+1.5$), as a function of the slope of the slow nullcline ($1/b$). Frequencies are given in hertz, considering a time step of 1 millisecond. Current intensities have no units. Other parameters of the Izhikevich model in Eqs. (4) are $a=0.02$ and $c=-65$.

ing rate of the neuron on the level of constant external current injected. The gain function of the Izhikevich model for different values of parameter b is presented in Fig. 3. Sensitivity is expressed as the increase in firing rate per unit of injected current, i.e., the average slope of the gain function. Clearly, the lower b is, the more sensitive the neuron.

Phase plane considerations immediately explain this dependence. In the nullcline diagram of Fig. 1, modifications of the current parameter I_v shift the fast nullcline (the parabola) horizontally. This alters the dynamics most if the slow nullcline is heavily slanted; if it is rather horizontal, shifting the fast nullcline has little effect on the phase plane configuration. The extreme case of this is the Rulkov model: The slope of the slow nullcline is zero, and step changes in I_v produce only transient effects. The gain function of the Rulkov model is zero.

This intuitive explanation can be confirmed analytically in the subthreshold regime, where we can make use of the generic equations (1) or their continuous-time equivalent (6). Below threshold there is no firing rate to refer sensitivity to, but we can redefine it as the amount of change in the resting voltage level when we inject current; this is nothing other

than the dc impedance of the neuron. If v^* is the resting voltage, i.e., the value of v at the fixed point, it is straightforward to derive, either from Eqs. (1) or Eqs. (6), that

$$S_{\text{subth}} \equiv Z(f=0) = \frac{\delta v^*}{\delta I_v} = \frac{1}{1 - f'(v^*) + p/q}. \quad (7)$$

This value is positive for all meaningful choices of $f(v)$ (injection of current should depolarize the neuron) and therefore sensitivity will be higher for lower values of p/q. But this is the inverse of the slope of the slow nullcline in the system of Eqs. (1) or Eqs. (6). Thus again sensitivity is tuned by this model feature. In the limiting case of the Rulkov model, $p/q = \infty$ and $S_{\text{subth}} = 0$.

Resonance

Resonance refers to the ability of the neuron to respond selectively to the frequency of external stimulation. In a classical setting, the external stimulation consists of a small sinusoidal input and the response is measured in terms of the amplitude of the induced oscillations or, in the case of a neuron model, also in terms of the modulation of the firing rate. This kind of resonance, that we will call *sinusoidal*, has been studied in [3] for the same generalized integrate-and-fire models we are using; we will briefly present a similar result in the context of the opposition between sensitivity and resonance. Nevertheless, sinusoidal stimulation has limited appeal in neuroscience, because by itself it is not realistic and because neurons are highly nonlinear systems whose response cannot be predicted from spectral decomposition. More interesting is stimulation by current pulses mimicking postsynaptic potentials. The selectivity of the neuron to the rate of incoming pulses is closely related to the presence of intrinsic subthreshold oscillations [2]: Pulses separated by an interval close to the subthreshold oscillation period will see their effect accumulated, while otherwise they will oppose or cancel each other. We therefore study the presence of damped and sustained subthreshold oscillations as indicative of *pulse resonance*. Pulse and sinusoidal resonance are linked. For example, intrinsic slow-decaying oscillations, necessary for pulse resonance, are the hallmark of classical underdamped resonant oscillators. Also note that spontaneous sustained subthreshold oscillations are the extreme form of sinusoidal resonance, since they correspond to an infinite gain exclusively at the oscillation frequency. Thus the two measures of resonance are related to each other and, not surprisingly, we will find that they show the same trend with the variation of model parameters.

We begin with sinusoidal resonance. A quiescent neuron subject to weak sinusoidal current injection will oscillate at the forcing frequency. Impedance curves $|Z(f)|$, depicting the quotient between the amplitude of the voltage response and that of the injected current for different frequencies, show a prominent peak for resonant neurons. In [3] a thorough analysis of these forced subthreshold oscillations is performed for the generalized integrate-and-fire model, which carries over, with straightforward changes of variables, to our generic models (1) and (6). An analytical expression for $Z(f)$ in terms of p, q, and $f'(v^*)$ (where v^* is the resting
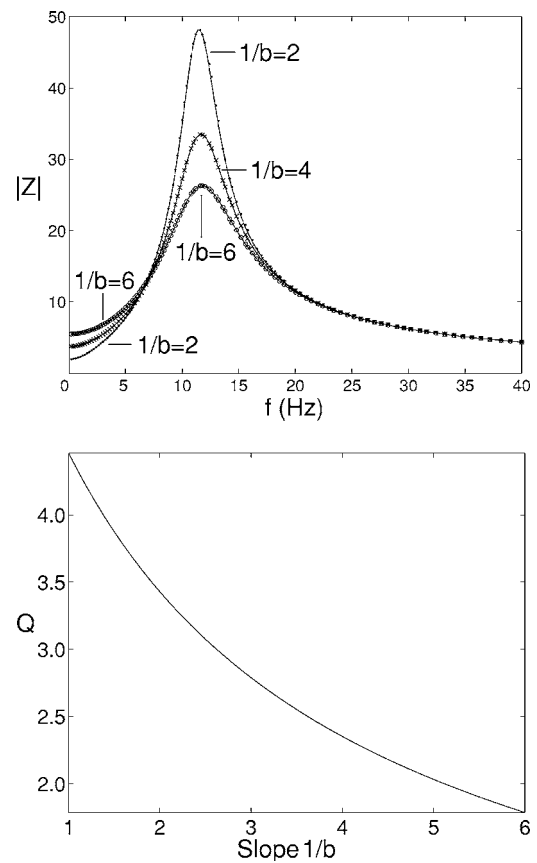

FIG. 4. Top: Impedance curves for the Izhikevich model at a resting potential $v^* = -62.7$ for different values of $1/b$, keeping $\omega^2 = a(b-a)$ constant at 0.005. The impedance has been calculated analytically through linearization (continuous line) and measured through simulation by injecting a sinusoidal current of amplitude $I_v = 0.001$ (dots, crosses, and circles). Bottom: Q value of the impedance curves as a function of $1/b$ under the same conditions.

voltage level) can be obtained but is too cumbersome to derive useful conclusions from it. We show rather, in Fig. 4, the impedance curves for the particular case of the Izhikevich model, for different values of the slope of the slow nullcline, $1/b$. For the sake of clarity, along with b we have modified a so as to keep the Neimark-Sacker frequency $\omega = \sqrt{ab - a^2}$ constant; this makes the resonant frequency almost independent of b and simplifies the visual comparison between the impedance curves. The standard measure of resonance, the Q value, is also presented. It is the ratio between the frequency of maximum impedance and the bandwidth at half power, i.e., the difference in frequency between points at $1/\sqrt{2}$ of maximum impedance. Clearly, the Q value, and thus resonance, decreases with increasing $1/b$, showing a trend opposite to that of sensitivity.

Note also that $|Z(0)|$ is the subthreshold sensitivity S_{subth} presented in Eq. (7). See in Fig. 4 how the curve with the sharpest resonance peak has the lowest value of $|Z(0)| = S_{\text{subth}}$ and vice versa. This is a nice depiction of the sensitivity versus resonance trade-off.

We turn now to pulse resonance. Figure 5 illustrates the concept. Short low-amplitude pulses similar to excitatory postsynaptic potentials are delivered at a certain rate to a
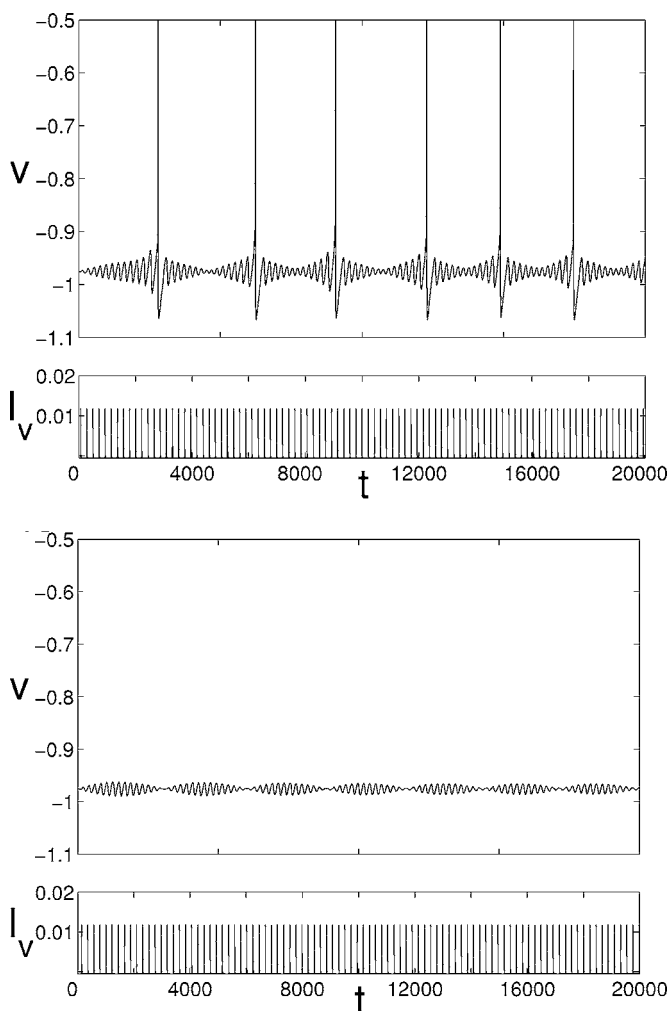
FIG. 5. Pulse resonance in the Rulkov model of Eqs. (2). Short, weak alpha-function shaped pulses are delivered to the neuron periodically. When their period precisely matches that of subthreshold oscillations, their effect accumulates and spikes are produced (top, $T_{pulses}=216$). A slight mismatch results in subthreshold beats (bottom, $T_{pulses}=218$). Observe that, in the matching case, after each spike the phase of the oscillations has changed and a phase realignment period follows. Neuron parameters are $\alpha=0.95$, $\mu=0.001$, and $\sigma=0.024$. Pulse parameters are $A=0.1$, $\tau=3$; see Eq. (11).

quiescent, excitable Rulkov neuron. They induce subthreshold oscillations and, if the pulse period is very similar to the oscillation period, their effect accumulates and spiking ensues. A frequency mismatch between pulses and subthreshold oscillations will instead produce beats. The point to bear in mind is that the damping of the oscillations determines the selectivity to pulse frequency, because if damping is strong, the oscillation elicited by a pulse will have mostly died out when the next pulse arrives, and thus the precise time of arrival will make little difference. For this reason we are going to study the damping of subthreshold oscillations, and afterwards measure its effect on pulse resonance.

Stable self-sustained subthreshold oscillations are the extreme case. They can be found, for example, in the Rulkov model of Eqs. (2): As σ is increased, the fixed point of the map loses stability through a supercritical Neimark-Sacker

bifurcation and small oscillations, in the form of a quasiperiodic solution on a small invariant closed curve, appear at a frequency given by the phase of the eigenvalues crossing the unit circle. These oscillations blow up into full-fledged spiking when σ is increased further. In contrast, in the Izhikevich model, for typical values of the parameters [6], the Neimark-Sacker bifurcation is subcritical, and the neuron switches directly from quiescence to spiking without the intermediate self-sustained subthreshold oscillation regime. Where does this difference stem from? Not from the fast subsystem, since the two models are locally identical in that regard, i.e., quadratic in the fast variable and linear in the slow variable. The difference lies rather in the slow variable dynamics, and again we are going to see that a low value of the slope of the slow nullcline enhances resonance.

Indeed, let (v^*, u^*) be a fixed point in the generic system (1). The necessary condition for loss of stability via a Neimark-Sacker bifurcation is

$$f'(v^*) = \frac{1-p}{1-q}, \quad \omega^2 \equiv p - q^2 > 0. \tag{8}$$

Note that with $p \approx q \ll 1$, the condition $p - q^2 > 0$ is always satisfied. The criticality of this bifurcation depends on the first Lyapunov coefficient, l_1, which can be easily calculated for a two-dimensional system [14] as follows:

$$l_1 = \frac{1-q}{8p}\left[f'''(v^*) - \left(1 - \frac{1}{p/q - q}\right)(1-q)[f''(v^*)]^2\right]. \tag{9}$$

If $l_1 > 0$ the bifurcation is subcritical, while, if $l_1 < 0$, it is supercritical. Therefore, for the existence of subthreshold oscillations the term in $[f''(v^*)]^2$ must be as large as possible. Since $p/q - q > 0$ according to the condition in Eq. (8), this is equivalent to requiring that p/q, the inverse of the slope of the slow nullcline, be as large as possible. Therefore, the flatter the nullcline, the more likely it is that the model presents self-sustained subthreshold oscillations.

The result is the same in the continuous-time case of Eqs. (6). The necessary condition for the Hopf bifurcation of the equilibrium point (v^*, u^*) is

$$f'(v^*) = q, \quad \omega^2 \equiv p - q^2 > 0,$$

and the first Lyapunov coefficient turns out to be

$$l_1 = \frac{1}{8p}\left[f'''(v^*) + \frac{1}{p/q - q}[f''(v^*)]^2\right].$$

In contrast with the discrete-time model, l_1 cannot be negative unless $f'''(v^*)$ is also negative; but, when this is the case, it is also necessary for the supercriticality of the bifurcation that p/q be as large as possible, i.e., that the slow nullcline be close to flat in the u-v diagram. It is worth noting that the Hopf bifurcation of the original, continuous-time form of the Izhikevich model, where $f'''(v^*)=0$, is inevitably subcritical, while in its discrete-time counterpart it can be made supercritical for a sufficiently horizontal slow nullcline, as will be shown in Fig. 6.

Damped oscillations appear before the loss of stability of the fixed point. Indeed, before going through either a subcritical or a supercritical Neimark-Sacker bifurcation, a
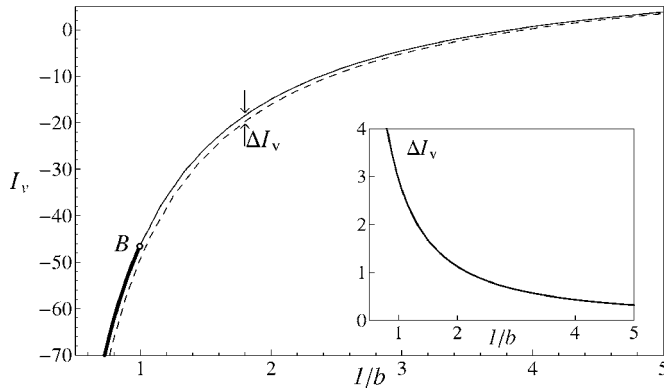
FIG. 6. Bifurcation diagram of the discrete-time Izhikevich model for parameters I_v and $1/b$, with $a=0.02$. The thick and thin continuous lines represent supercritical and subcritical Hopf bifurcations, respectively. The circle denoted by B is the Bautin point where criticality changes. The dashed line has constant logarithmic damping $\ln K=-10$. Inset: Difference in currents between the Neimark-Sacker bifurcation curve and the constant logarithmic damping line as a function of $1/b$.

stable fixed point, with two complex eigenvalues, is a spiral sink around which the orbit turns while falling into it. Although the resulting oscillations are not sustained, they may take a large number of turns to die, and endow the neuron with the same selectivity properties as sustained oscillations do. The amount of damping can be quantified by the damping factor K, which is the ratio between the amplitude of two consecutive free small oscillations. Its value is readily obtained from the eigenvalues of the fixed point as follows:

$$K = e^{2\pi \, \mathrm{Re}(\lambda)/|\mathrm{Im}(\lambda)|} \quad \text{in continuous-time systems,}$$

$$K = |\lambda|^{2\pi/|\arg(\lambda)|} \quad \text{in discrete-time systems,}$$

where λ is any of the two conjugate eigenvalues. The closer K is to 1, the less damped the oscillations are, and the more pronounced the resonance effects can be expected to be.

For any choice of parameters p and q in the generic models (1) and (6), K covers all the values up to 1 as the external input I_v drives the neuron towards the Neimark-Sacker or Hopf bifurcation; we cannot use the value of K by itself to discriminate more or less resonant models. But in some cases K remains very close to unity through a wide range of values of I_v, while in others I_v must be very finely tuned below threshold to observe a significantly slow damping. Thus, an interesting measure of the ability to produce long-lasting subthreshold oscillations is the range of I_v between a certain fixed value of $K<1$ and $K=1$, the bifurcation point. In addition, this highlights the trade-off between oscillations and sensitivity to external inputs. The bifurcation diagram in Fig. 6 presents such a measure for the discrete-time Izhikevich model (4). In this diagram, $1/b$, that is, the slope of the slow nullcline, and I_v are the free parameters. The continuous line represents the Neimark-Sacker bifurcation of the fixed point. It changes from supercritical to subcritical at the Bautin point B, where the first Lyapunov coefficient l_1, as given in Eq. (9), is zero. The dashed line is not a bifurcation curve but a set of

parameter values corresponding to a constant value of damping K. As $1/b$ is increased and correspondingly the slow nullcline becomes more slanted, the interval of the current ΔI_v between the two curves decays, as shown in the inset; consequently, the external input must be more finely tuned to produce subthreshold oscillations. At the same time, the need of ever-smaller increases of current to jump from damped oscillations to spiking reveals the growing sensitivity to external excitation, as we discussed previously. The trade-off becomes apparent: Increased sensitivity reduces the aptitude for resonance. It can also be observed that the supercritical Neimark-Sacker bifurcation corresponds to the lower values of $1/b$ and vice versa: Self-sustained intrinsic oscillations are present for the parameter values that make damped oscillations longer lasting.

The damping analysis performed above on the Izhikevich model (4) can be generalized to both generic models (1) and (6) under mild assumptions on $f(v)$. For example, in the continuous case (6), since the eigenvalues of the equilibrium point satisfy $\tau(\lambda_1+\lambda_2)=f'(v^*)-q$ and $\tau^2\lambda_1\lambda_2=p-qf'(v^*)$, it is easy to find the conditions for the Hopf bifurcation and for a damping value $K=e^{-2\pi}$:

$$f'(v^*)|_{\mathrm{Hopf}} = q,$$

$$f'(v^*)|_{K=e^{-2\pi}} = -\sqrt{2p-q^2}.$$

On the other hand, from Eqs. (6), we obtain the variation of $f'(v^*)$ with respect to the external current I_v as follows:

$$\frac{\delta f'(v^*)}{\delta I_v} = \frac{qf''(v^*)}{p-qf'(v^*)}.$$

We can invert and integrate the preceding expression to obtain the current interval ΔI_v between damping $K=e^{-2\pi}$ and the Hopf bifurcation:

$$\Delta I_v = \int_{-\sqrt{2p-q^2}}^{q} \frac{p-qf'(v^*)}{qf''(v^*)} df'(v^*)$$

$$= \frac{p(\sqrt{2p-q^2}+q)}{qf''(\xi_1)} + \frac{p-q^2}{f''(\xi_2)}, \tag{10}$$

where ξ_1 and ξ_2 are values of the voltage intermediate between the value v^* at the Hopf bifurcation and the value that corresponds to the damping $K=e^{-2\pi}$. As long as $f''(v)$ does not vary too sharply in the intervals considered [in the case of the quadratic Rulkov and Izhikevich models, $f''(v)$ is constant], and taking into account that $p-q^2>0$, both terms in the right-hand side of Eq. (10) are increasing with p/q, the inverse of the slope of the slow nullcline. Therefore a wider margin of I_v for long-lasting damped oscillations results from a flatter nullcline, which at the same time entails reduced sensitivity to external excitation.

We are now in a position to directly test pulse resonance as a function of parameters. We stimulate a quiescent neuron with very short current pulses at different frequencies and measure the minimum amplitude of the pulses necessary to elicit a spike. The inverse of this amplitude we call the pulse impedance, Z_{pulse}. A high pulse impedance is found at resonant frequencies, and it means that very weak pulses are able
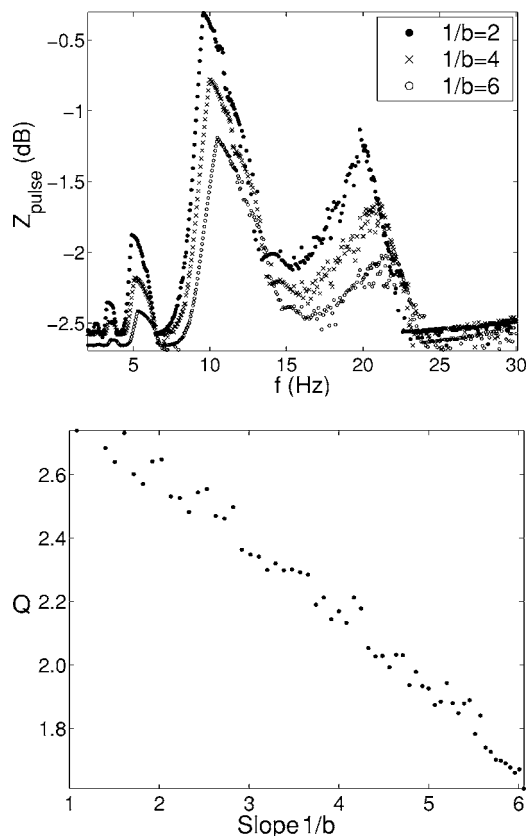
FIG. 7. Top: Pulse impedance curves (see text for definition) in the Izhikevich model for different values of $1/b$, keeping $\omega^2 = a(b-a)$ constant at 0.005. Impedance has been measured at a resting potential $v^* = -62.7$ in all cases. Pulses used are alpha functions with $\tau = 3$ ms; see Eq. (11). Bottom: Q value of the pulse impedance curves as a function of $1/b$ under the same conditions.

to induce an action potential by accumulation along several periods. Figure 7 represents pulse impedance as a function of pulse frequency in the discrete Izhikevich model, Eqs. (4), for different values of the slope of the slow nullcline. The figure is the pulse analogue to the sinusoidal resonance curves of Fig. 4, and, as we did there, for ease of comparison, we have modified a along with b to keep the resonant frequency constant around 10 Hz. As with sinusoidal resonance, the impedance peaks are sharper for the smaller values of the slope $1/b$. Observe the secondary resonant peaks at half, one-third, etc. frequency of the main peak, where the difference in sharpness is even more noticeable. This is to be expected because damping controls pulse resonance, and its effect is stronger for pulses delivered every two, three, etc. oscillations. The less expected secondary peak at *double* frequency of the main peak is due to entrainment, and indeed our pulse impedance curves can be seen as (inverted) Arnold tongues [15]. Finally, at high frequencies Z_{pulse} values become noisy due to sampling limitations.

To quantify the sharpness of the resonant peaks we have calculated the Q value at 1 dB of the peak. It is also presented in Fig. 7. The same trend of higher Q value for the flatter slopes results, as expected.

IMPLICATIONS FOR NEURON FUNCTIONALITY

The preceding discussion leads to the following conclusion: There is a trade-off between the sensitivity to external currents (integrator behavior) and the selectivity with respect to the frequency of stimulation (resonator behavior) in two-dimensional spiking-bursting models with fast and slow time scales. If the slow variable is strongly stable, the model will be very sensitive to external inputs, but unable to sustain subthreshold oscillations. If, on the other hand, the slow variable is close to neutrality, stable or long lasting oscillations will be observable, frequency selectivity will be sharper, but the response to changes in external currents will be dampened.

We have derived this result from the analysis of the subthreshold dynamics of an isolated neuron, and illustrated it with mathematically simple stimuli such as step, sinusoidal, and periodic pulsed currents. But we still have to show that it is relevant for the functionality of the neuron, in its response to complex stimuli and its interaction with other neurons. In this section, we show the implications of the aforementioned trade-off, evaluating them through simulations in the excitable, spiking, and bursting regimes.

Excitable regime

Neurons are said to be in the *excitable regime* if they are silent but close enough to loss of stability as to produce single action potentials when pushed slightly away from equilibrium. In this regime, neurons are most sensitive to external input, but this sensitivity is strongly dependent on the stability of the slow variable of the model, as we shall presently show through simulations.

We use the discrete-time Izhikevich model of Eqs. (4) with different values of the slow nullcline slope $1/b$. A stationary current $I_v(b)$ is injected such that the resting voltage of the system is stable at $v^* = -62.7$ for all values of b, i.e., the intersection between both nullclines is in all cases at the same point of the parabolic fast nullcline. This equilibrium being stable, the neuron is silent but close to losing stability, i.e., excitable. We have used this setting before to measure resonance curves. But in this case we will add to I_v a small Gaussian white noise and synaptic stimulation consisting of a zero-mean Poissonian train of alpha functions

$$\alpha(t) = \frac{A}{\tau^2} t e^{-t/\tau}. \tag{11}$$

Zero mean is obtained by combining excitatory and inhibitory currents, i.e., positive and negative values of amplitude A. The decay time of the alpha functions is $\tau = 5$ ms and the mean period of the Poisson process is 30 ms. Subject to this noisy input, the neuron fires irregularly. This corresponds to the high noise regime described in [3], where the autonomous resonance frequency of the neuron is dominant. We measure two quantities: The coefficient of variation of the interspike intervals T, i.e., $C_V = \sigma_T/\langle T \rangle$, and the sensitivity measured from the gain in spiking rate relative to increases in the Poissonian stimulation amplitude. Figure 8 shows the result.
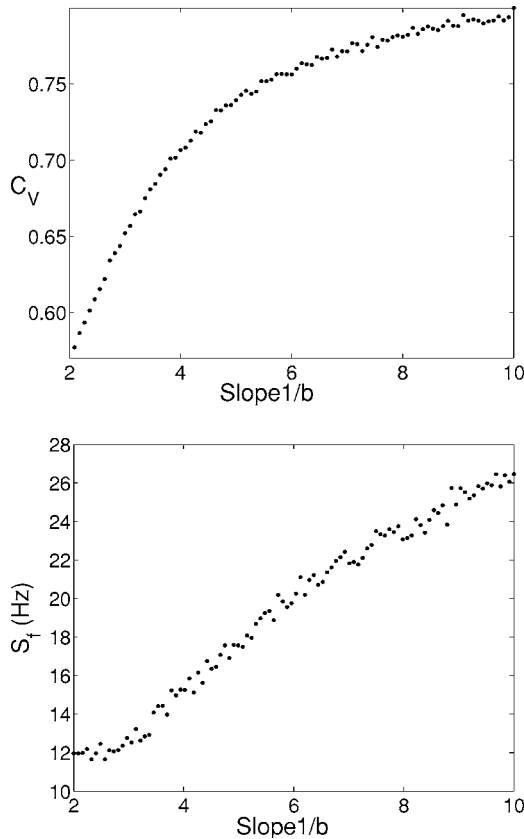
FIG. 8. Coefficient of variation C_V (top) and sensitivity of the spiking frequency S_f (bottom) for different values of $1/b$ in the Izhikevich model (4) stimulated by a Poissonian input and Gaussian white noise. In the C_V figure, each point corresponds to the average of 100 realizations of noise. In the S_f figure, values have been calculated from linear regression of the average firing rate of the neuron against alpha function amplitudes between 1 and 2.5. Other parameters are $a = 0.02$ and $c = -62.5$.

First it can be observed that the coefficient of variation is less than unity, which is the C_V of the stimulation. Therefore, the neuron regularizes the input stimulus. This is to be expected simply as a result of refractoriness [13]. The interesting point is that the degree of regularization decreases (C_V increases) with increasing $1/b$. This is due to the loss of resonance described in the previous section. Indeed, the Poisson input is to pulse stimulation as white noise is to sinusoidal stimulation, and C_V is a measure of how effective the neuron is as a pulse filter (the lower C_V, the more effective). On the other hand, along with the increase in C_V, sensitivity also increases. The reason is, as explained before, that a steeper slope of the slow nullcline ensures that the fixed point is more easily modified by external excitation of the fast variable. The trade-off between resonator and integrator capabilities becomes apparent.

Regular spiking regime—synchronizability

When the external current is strong enough, neurons enter the regular spiking regime, where action potentials are generated with a constant period. A network of identical neurons

subjected to the same constant external current will fire with a uniform period, though, under random initial conditions, they will not fire synchronously. If the neurons are diffusively coupled through electrical synapses, and the coupling is strong enough, dephasing will disappear and perfect synchronization will be achieved. Electrical synapses are known to play a fundamental role in synchronizing neurons in mammalian central nervous system structures such as the brain stem, the inferior olive, and the hippocampus, and are also ubiquitous between interneurons in the neocortex, although their role there remains still unclear. Studying the interplay between intrinsic currents and gap junction connections is necessary to understand why electrical synapses are present in certain types of neurons and how they help to achieve synchronization [16].

Therefore we set out to measure how synchronizability between electrically coupled neurons is affected by changes in the slope of the slow nullcline of our neuron models. Synchronizability can be measured by the minimum coupling strength required to obtain complete synchronization of the network: The stronger the necessary coupling, the smaller the synchronizability. In order to make this measure independent of network topology, we resort to the master stability function of the model to separate the network modes [17]. With this technique, the following coupled generic system of N neurons

$$v_n(t+1) = f(v_n(t)) - u_n(t) + I_v + \sum_{m=1}^{N} g_{mn}(v_m(t) - v_n(t)),$$

$$u_n(t+1) = u_n(t) + pv_n(t) - qu_n(t) + I_u, \quad n = 1, 2, \ldots, N,$$

$$(12)$$

can be linearized around the synchronized trajectory and diagonalized to obtain N independent, two-dimensional subsystems:

$$\begin{bmatrix} \xi_{v,n}(t+1) \\ \xi_{u,n}(t+1) \end{bmatrix} = \left(\begin{bmatrix} f'(v(t)) & -1 \\ p & 1-q \end{bmatrix} + \lambda_n \begin{bmatrix} 1 & 0 \\ 0 & 0 \end{bmatrix} \right) \begin{bmatrix} \xi_{v,n}(t) \\ \xi_{u,n}(t) \end{bmatrix},$$

$$(13)$$

where $\lambda_1 = 0 > \lambda_2 > \cdots > \lambda_N$ are the eigenvalues of the matrix of diffusive connections g_{mn}. Stability in the total system is ensured if all modes are stable except, possibly, the first one, which is parallel to the synchronization manifold. Since all eigenvalues, except $\lambda_1 = 0$, of the diffusive connectivity matrix are negative, their effect on each subsystem is stabilizing. We can now give a precise, network-independent measure of synchronizability: The maximum value $\lambda_{\max}$ which, when substituted for λ_n in Eq. (13), makes the maximum Lyapunov exponent of the mode along the synchronized periodic trajectory negative. When this happens, trajectories near the synchronized orbit shrink towards it at an exponential rate and thus the synchronized orbit is stable. The diffusive characteristic of the coupling guarantees that the same synchronized trajectory is a solution of the system for all values of coupling.

We perform such measure of synchronizability on the Izhikevich model (4) with diffusive coupling, for different
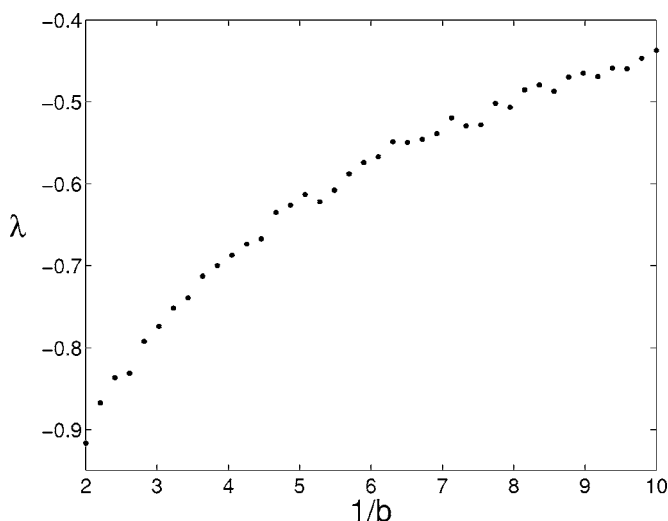
FIG. 9. Synchronizability λ_{max} of the Izhikevich model for different values of the slow nullcline slope, $1/b$. The external current I_v is such that the fixed point is at $v^* = -62$ in all cases. The other parameters are $a = 0.02$ and $c = -62.5$.

values of the slope of the slow nullcline $1/b$. The result is shown in Fig. 9. Synchronization is easier for higher values of $1/b$, where sensitivity to external currents is higher. It is worth noting that subthreshold oscillations, which are produced for *lower* values of $1/b$, do not enhance synchronizability. This is because synchronization through diffusive coupling is achieved more easily when neurons are responsive to each other's voltage, rather than follow their own internal oscillatory dynamics.

Bursting regime—chaotic itinerancy

Finally we point out another consequence of the subthreshold behaviors of the models, i.e., the modulation of *chaotic itinerancy* [18,19]. Chaotic itinerancy is a dynamic regime in which a system switches back and forth between ordered motions around so-called "attractor ruins" and chaotic transients linking these ordered motions. In a network of neurons this phenomenon can manifest itself as the chaotic alternation of regular activity patterns such as standing and rotating waves [7].

In order to observe chaotic itinerancy we take the variant of the Rulkov model designed specifically for chaotic bursting [10], whose equations are as follows:

$$v(t+1) = \frac{\alpha}{1 + v(t)^2} + u(t) + I_v,$$

$$u(t+1) = u(t) - \mu(v(t) + au(t) - \sigma). \tag{14}$$

Again this is our generic model of Eqs. (1), with $p = \mu$, $q = \mu a$, and $I_u = \mu\sigma$. The return map $F(v, I_v + u)$, depicted in Fig. 2(c), replaces the hard reset mechanism of other models by a smooth unimodal function. This is the source of the chaotic bursts. Observe that the slope of the slow nullcline is $q/p = a$. Parameter a is zero in the original model, which, as all the variants of the Rulkov model, has a horizontal slow

nullcline. With $a > 0$ we modify the slope and, according to the analysis performed on the generic model (1), tune the sensitivity versus resonance trade-off.

In a previous paper [7], we have shown that a regular network composed of this type of model exhibits chaotic itinerancy for certain values of coupling parameters. We investigate now its dependence on the slope of the slow nullcline. To this end we couple the neurons through inhibitory connections as in Ref. [7]. The resulting system is

$$v_n(t+1) = \frac{\alpha}{1 + v_n(t)^2} + u_n(t)$$

$$- g_c \sum_{m=1}^{N} \gamma_{mn}(v_m(t) - \nu)H(v_m(t) - \nu),$$

$$u_n(t+1) = u_n(t) - \mu(v_n(t) + au_n(t) - \sigma), \tag{15}$$

where $H(v)$ is the Heaviside step function, $g_c > 0$ represents the strength of inhibitory coupling, the γ_{mn}, valued 0 or 1, determine the topology of the network, and ν is the presynaptic threshold of synaptic interaction. In Ref. [7] we used master stability functions to show, for the case $a = 0$, that bursting is emergent in this setting. Emergent bursting means that the minimum excitation σ needed to produce bursts in the coupled system is smaller when neurons are coupled than when they are isolated [20]. When σ is well above the threshold for bursting, activity is completely chaotic, while if σ is barely above the threshold, a chaotic alternation of ordered modes of activity appears instead. All this carries over for positive values of a, but, as can be seen in Fig. 10, higher values of a produce less orderly patterns of activity.

We quantify this loss of order by measuring the dependence of autocorrelation on the value of a. One of the most salient features that characterize chaotic itinerancy is the slow decay of correlations in the activity of neurons, which corresponds to the order in each of the modes that alternate along the itinerant orbit. Figure 11 shows, on the left, the average autocovariance of the voltages of the 32 neurons in the ring for two different values of a. Clearly, correlations are stronger for lower a. On the right we present, as a function of a, the signal-to-noise ratio (SNR) of the network calculated from the power spectrum as the ratio between the peak around the mean bursting period and the noise level at high frequencies. The SNR measures the amount of periodicity in the autocorrelations, and thus the temporal regularity of the network activity. We see that when a is small the SNR is high, and thus correlation is stronger, but it decreases with increasing a, corresponding to weaker and faster-decaying correlations. This is in agreement with the intuitive appreciation of Fig. 10.

We try to interpret this result in the light of our previous discussion. A higher value of a means loss of neutral stability of the slow variables of the neurons, which is accompanied by loss of subthreshold resonance and increased current sensitivity. The neutrality of slow variables means that the system has many near-zero Lyapunov exponents, which is a necessary trait of chaotic itinerancy [18]. This allows for the appearance of the characteristic low-dimensional attractor ru-
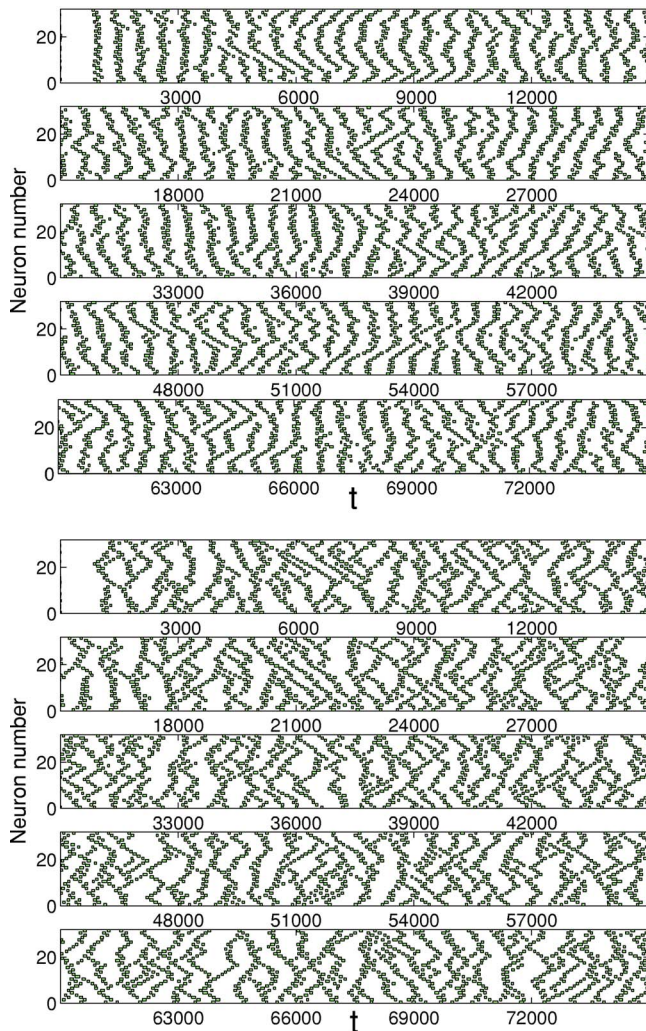
FIG. 10. (Color online) Chaotic activity in a ring of $N=32$ Rulkov neurons following Eqs. (15) with $a=0.5$ (top) and $a=4.5$ (bottom). Excitation σ is such that mean activity is roughly the same in both cases, with bursts every 600–700 time units. Other parameters are $\alpha=4.3$, $\mu=0.001$, $\nu=-2.5$, and $g_c=0.01$.
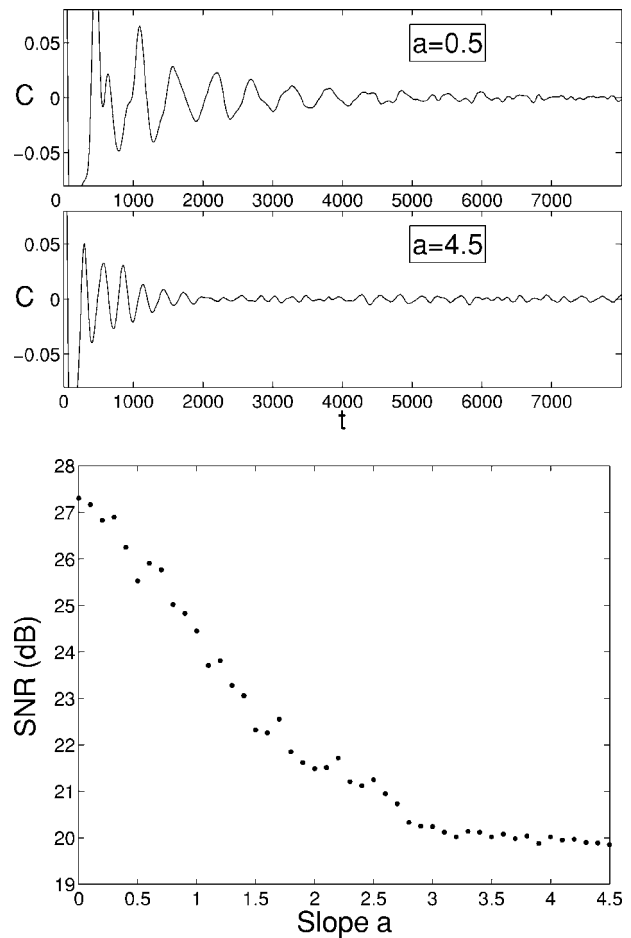

FIG. 11. Top: Average autocovariance $C(t)$ of the fast variable of the 32 neurons in the simulation of Fig. 10 corresponding to $a=0.5$. Middle: The same for $a=4.5$. Bottom: Signal-to-noise ratio, plotted against a, of the average activity of the Rulkov neurons, measured as the ratio between the power spectrum peak around the average bursting frequency and the power spectrum level at high frequencies. All the parameters other than a are the same as in Fig. 10.

ins corresponding to the ordered modes. When a is increased, near-zero Lyapunov exponents shift away from zero and low-dimensional modes merge into complex chaotic patterns. Nevertheless, this explanation is tentative until we perform a detailed analysis of the chaotic attractors of this system.

CONCLUSION

The choice of an appropriate model, with the right set of parameters, to investigate the behavior of networks of neurons is one of the most important steps in neuroscientific modeling. Our purpose in the present work has been to gain insight into the consequences of an important property of simple phenomenological models: The neutral or asymptotic character of the slow variables. We have shown how phase plane and bifurcation analysis explains the influence of this feature on the dynamics of the model. A neutral slow vari-

able is the best choice for resonance, although it entails a loss of sensitivity to external steady currents. This trade-off has a wide range of consequences including the negative effect of resonance upon synchronizability. Also interesting are its effects on chaotic dynamics, the elucidation of which, however, needs further elaboration. We will address this problem in our future research.

When higher dimensional, more realistic models are employed, our analysis can be directly applied only after an appropriate reduction of dimension is carried out [21]. For example, the three-dimensional Hindmarsh-Rose model [22] is amenable to dimension reduction by averaging its fast gating variable to obtain a nonspiking model under the form of our generic model (6). In many other cases, however, such reduction is not possible without loss of significant sub-threshold characteristics. For example, two-variable models cannot reproduce the bimodal frequency response found in some hippocampal interneurons [3,23]. Characterization of the features and trade-offs of higher dimensional models still offers a wide field of research.

[1] J. Rinzel and G. B. Ermentrout, in *Methods in Neuronal Modeling: from Synapses to Networks*, edited by C. Koch and I. Segev (MIT Press, Boston, 1989), pp. 135–169.

[2] E. M. Izhikevich, Neural Networks **14**, 883 (2001).

[3] M. J. E. Richardson, N. Brunel, and V. Hakim, J. Neurophysiol. **89**, 2538 (2003).

[4] E. M. Izhikevich, Int. J. Bifurcation Chaos Appl. Sci. Eng. **10**, 1171 (2000).

[5] A. L. Shilnikov and N. F. Rulkov, Phys. Lett. A **328**, 177 (2004).

[6] E. M. Izhikevich, IEEE Trans. Neural Netw. **14**, 1569 (2003).

[7] G. Tanaka, B. Ibarz, M. A. F. Sanjuán, and K. Aihara, Chaos **16**, 013113 (2006).

[8] J. M. Casado, B. Ibarz, and M. A. F. Sanjuán, Mod. Phys. Lett. B **18**, 1347 (2004).

[9] N. F. Rulkov, I. Timofeev, and M. Bazhenov, J. Comput. Neurosci. **17**, 203 (2004).

[10] N. F. Rulkov, Phys. Rev. Lett. **86**, 183 (2001).

[11] N. F. Rulkov, Phys. Rev. E **65**, 041922 (2002).

[12] E. M. Izhikevich, Int. J. Bifurcation Chaos Appl. Sci. Eng. **14**, 3847 (2004).

[13] W. Gerstner and W. M. Kistler, *Spiking Neuron Models* (Cambridge University Press, Cambridge, UK, 1999).

[14] J. Guckenheimer and P. Holmes, *Nonlinear Oscillations, Dynamical Systems and Bifurcations of Vector Fields*, Applied Mathematical Sciences Vol. 42 (Springer, New York, 1983).

[15] A. Pikovsky, M. Rosenblum, and J. Kurths, *Synchronization: A Universal Concept in Nonlinear Sciences*, Cambridge Nonlinear Science Series (Cambridge University Press, Cambridge, UK, 2003).

[16] B. Pfeuty, G. Mato, D. Golomb, and D. Hansel, J. Neurosci. **23**, 6280 (2003).

[17] L. M. Pecora and T. L. Carroll, Phys. Rev. Lett. **80**, 2109 (1998).

[18] K. Kaneko and I. Tsuda, Chaos **13**, 926 (2003).

[19] G. Tanaka, M. A. F. Sanjuán, and K. Aihara, Phys. Rev. E **71**, 016219 (2005).

[20] G. de Vries, Phys. Rev. E **64**, 051914 (2001).

[21] H. R. Wilson, *Spikes, Decisions and Actions* (Oxford University Press, New York, 1999).

[22] J. L. Hindmarsh and R. M. Rose, Proc. R. Soc. London, Ser. B **221**, 87 (1984).

[23] F. G. Pike, P. S. Goddard, J. M. Suckling, P. Ganter, N. Kasthuri, and O. Paulsen, J. Physiol. (London) **529**, 205 (2000).